ACS OMEGA

http://pubs.acs.org/journal/acsodf

Article

Boron Nitride Microspheres via Pyrolysis of Polymerized Precursors

Zexia Li, Jingwen Yang, Hejun Gao, Jiaxiao Qiao, Wei Qiao, Peng Wang, Jun Zhang, Chengchun Tang, and Yanming Xue*

Cite This: *ACS Omega* 2023, 8, 15239−15248

Read Online

ACCESS | Metrics & More | Article Recommendations | Supporting Information

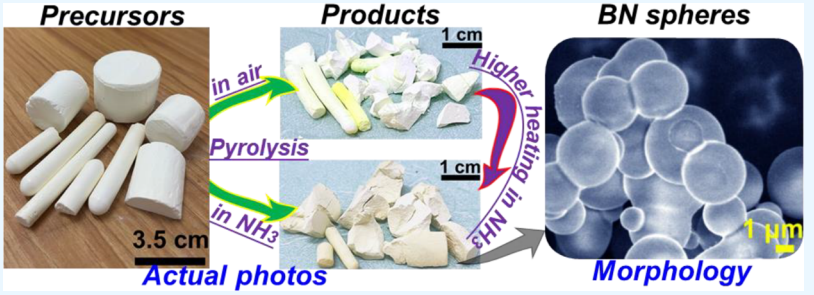

ABSTRACT: Microspheric BN materials have high application potential because they have better fluidity and dispersion ability to endow hexagonal boron nitride (h-BN) ceramics and h-BN/polymer composites with highly desired performance. In this work, a novel synthetic route to the BN microspheres has been developed by means of a controllable pyrolysis of polymerized spherical precursors. The precursor formation mechanism is proposed to be the F-127-induced self-assembling polymerization of a boric acid−melamine−formaldehyde (MF) colloid. It is found that ammonia-annealing of an air-pyrolysis (700 °C) intermediate causes higher BN phase transformation within final BN microspheres with more uniform diameter distribution compared to those of direct ammonia-pyrolysis of spherical precursors at the same temperatures of 1100 and 1500 °C. After ammonia-annealing and ammonia-pyrolyzed treatment at 1100 and 1500 °C, the obtained BN microspheres have a low specific surface area (SSA) property, but replacing part of melamine with dicyandiamide could increase their SSAs to more than 1000 m^2/g. We believe that this new microspherical BN preparation with more facile and controllable operation would be well suited for industrialization.

INTRODUCTION

A spherical boron nitride (BN) has better fluidity than its natural sheetlike morphology.[1] The use of spherical BN can improve the forming density of hexagonal boron nitride (h-BN) ceramics and enhance the mass transfer efficiency in a sintering process.[2,3] The BN spheres can easily achieve a well-uniform and highly dense filling within polymeric composites, thereby greatly enhancing the composite's mechanical and thermal properties.[4−6] Thus, it is of great significance to develop reliable large-scale preparation of spherical BN for ameliorating the performance of h-BN-based ceramics and BN-filled polymer composites.

Up to now, there have been several well-known synthetic routes to the spherical BN products. Most of them were mainly realized by the well nitrogenize reaction of the various B- and/or N-containing atomized droplets through the chemical vapor deposition (CVD) strategy.[7−11] Trimethyl borate was first used by Tang et al. as the atomized source.[7,8] They successfully synthesized a kind of quasi-nanospherical BN particles via the first-stage CVD reaction at 980 °C in ammonia for a spherical intermediate and the second-stage ammonia-annealing of the intermediate at 1400 °C. Wood's group pyrolyzed the aqueous atomized aerosols of guanidinium borates in the ammonia-assisted CVD system between 600 and 1400 °C, obtaining the microspherical BN particles.[9] However, these CVD processes have the disadvantages of difficult collection for samples, easy blockage to the gas path, poor controllability in the morphology, and low yield. By using a C sphere as a template, Terrones and co-workers prepared spherical BN via in-situ carbothermal reduction based on the nitrogen-assisted B−O vapor substitution reaction.[12] Due to the use of spherical C templates, these BN spheres easily had high C impurity.[12,13] Zhang et al. used borax and boric acid as B sources, urea as a N source, DTAC as a soft template, acryl amide as a monomer, *N*-methylene bis-acrylamide as a cross-linking agent, and ammonium persulfate as an initiator to form a microspherical precursor by performing a chemical reaction among them.[14] Although they claimed that a BN component could be formed within the microsphere depending ammonia treatment between 625 and 900 °C, the samples have a lot of various

Received: January 16, 2023
Accepted: April 3, 2023
Published: April 21, 2023

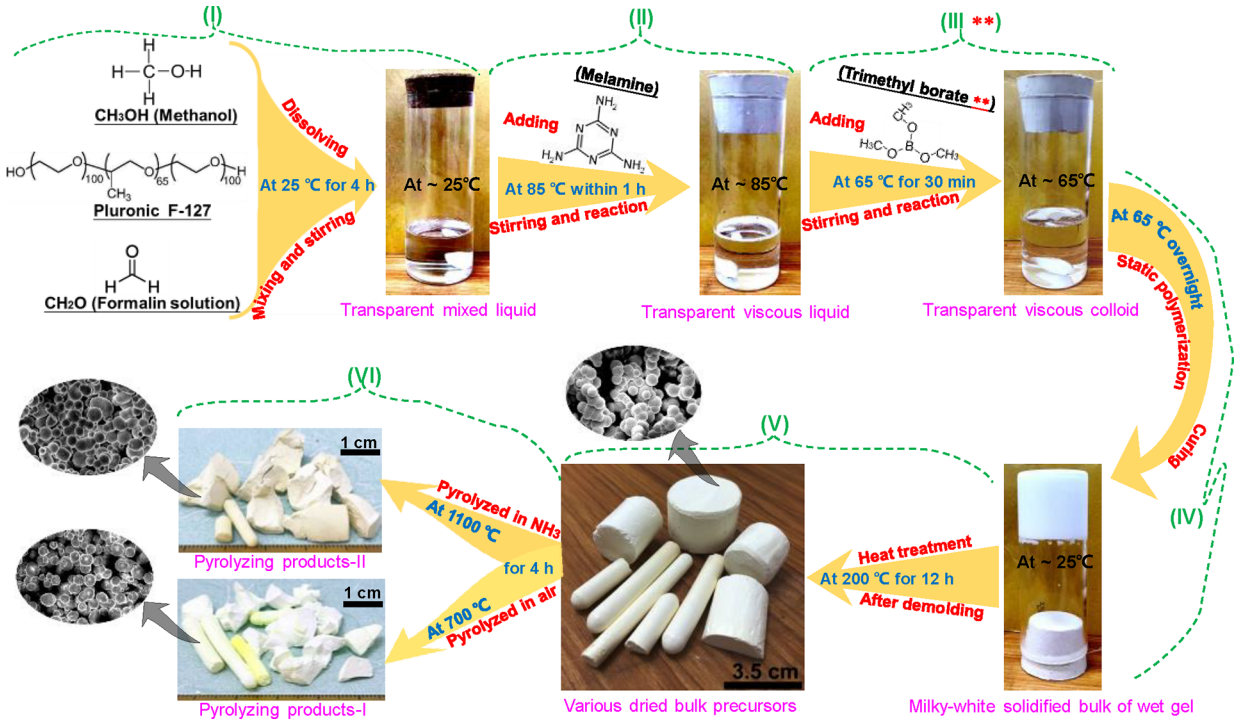

Figure 1. Synthetic route to BN microspheres and their architected bulk materials. Note: for the step III**, **means that, in this step, the boric acid was used to replace trimethyl borate without changing the subsequent steps, and the same products could be obtained. However, compared with trimethyl borate, the use of boric acid would make static polymerization and curing time much shorter in step IV.

impurities within them.[14,15] Multiple and complicated cleaning procedures must be implemented for the final purification of the BN samples. Zhang's report illustrated a polymer-chemical route to prepare BN microspheres with high-purity and narrow-dispersed properties at 1400 °C and under a nitrogen pressure of 3.0 MPa.[16] In fact, the poly-trichloroborazine (poly-TCB) precursor used by them is highly toxic, while its synthesis is very harsh and highly costly. Indeed, the abovementioned approaches are still challenging for large-scale production of BN spheres. Thus, it is necessary at present to develop novel spherical BN preparation with a facile, controllable, and industrializable route.

Herein, we have developed another large-scale synthetic route to the microspherical BN materials via two main processes including controllable colloidal polymerization of microspherical precursors and flexible pyrolysis of the precursors. The formation mechanism of the microspherical precursor was clearly proposed. Subsequently, the spherical BN obtained at different pyrolysis temperatures and atmospheres and different ammonia-annealing temperatures were investigated in detail. On the basis of the morphology, composition, and porosity results of samples, the pyrolysis and annealing processes from the precursor to BN microspheres were also analyzed. We believed that this novel preparation process is available for further commercialization.

EXPERIMENTAL SECTION

Synthesis of Precursors. F-127 (6 g) (Sigma-Aldrich Trading Co., Ltd. Shanghai) was completely dissolved into the mixed solution made of 10 mL of methanol (Shanghai Aladdin Biochemical Technology Co., Ltd.) and 20 mL of formalin solution (formaldehyde of 37 wt %, Shanghai Aladdin Biochemical Technology Co., Ltd.) to obtain a transparent mixed liquid with constant stirring for 4 h at room temperature (RT). Melamine (13 g) (Shanghai Aladdin Biochemical Technology Co., Ltd.) was dissolved into this above-formed liquid in an oil bath at 85 °C within 1 h to form a transparent viscous liquid. Trimethyl borate (TMB) (11 g) or 6.5 g of boric acid (BA) (Shanghai Aladdin Biochemical Technology Co., Ltd.) was added into the abovementioned viscous liquid with oil bath at 65 °C with stirring for 30 min to get a transparent viscous colloid. Then, the stirring operation was stopped, and static polymerization of the colloid was carried out in a container at 65 °C overnight to form a curing solidification bulk of wet gel. Furthermore, the wet solidification bulk was heated to 200 °C with a heating rate of 1 °C/min and kept for 12 h in an oven. Finally, the dried precursor bulk was obtained after the heating treatment and demolding from the container at RT.

Pyrolysis of Precursors and Annealing of Intermediates. The precursor bulk was pyrolyzed at 700 °C for 4 h in air to obtain the intermediate. The precursor bulk was directly pyrolyzed at 1100 and 1500 °C for 4 h in ammonia to obtain the BN microspheres. The intermediate was further annealed at 1100 and 1500 °C for 4 h in ammonia to also acquire the microspherical BN materials. The heating rate and gas flow rate of the abovementioned processes are 1−5 °C/min and 50 mL/min, respectively.

Characteristics. The morphology and structure of the samples were investigated and analyzed with scanning electron microscopy (SEM) (JSM-7610F, Japan), transmission electron microscopy (TEM), and high-resolution TEM (HR-TEM) (JEM-2100F, Japan). The X-ray diffraction (XRD) instrument (D8 Discover Bruker, Germany) was used to measure the crystal phase information of samples. The Fourier transform infrared (FTIR) spectra (WQF-410) were used to reveal the surficial chemical groups of the samples. The specific surface area (SSA) and pore size distribution of the samples were

https://doi.org/10.1021/acsomega.3c00313
ACS Omega 2023, 8, 15239−15248

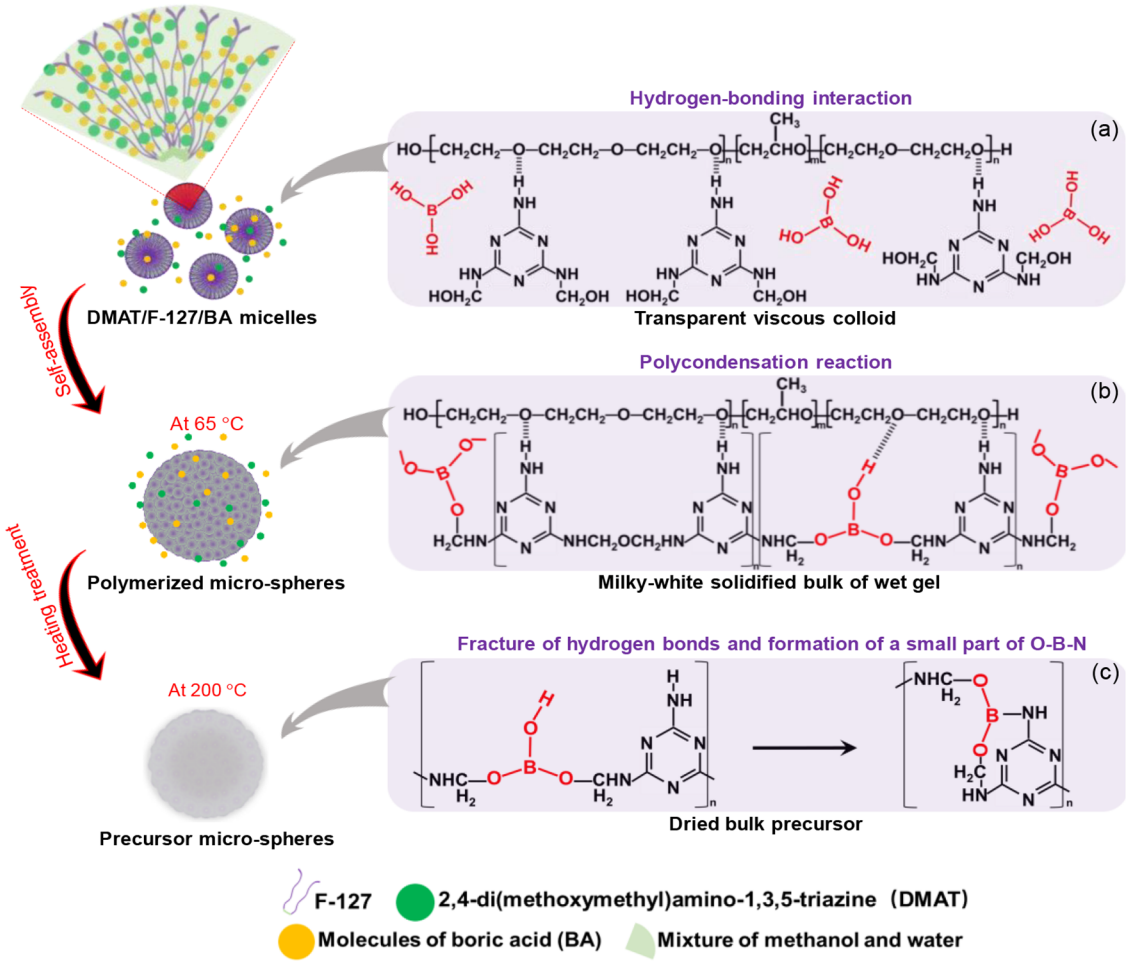

Figure 2. Formation mechanism of microspherical precursors. (a) Colloid formation. (b) Wet gel formation. (c) Dried bulk precursor formation.

acquired and analyzed by using an automatic physical and chemical adsorption isotherm (Quanta Chrome Autosorb-iQ) by using a quenched-solid density functional theory (QSDFT) and Brunauer–Emmett–Teller (BET) methods. Thermogravimetric analysis was performed by using an SDT Q 600 thermal analyzer, with a heating rate of 5 °C/min in air flow. The measurements of X-ray photoelectron spectroscopy (XPS, ESCALAB 250Xi, Thermo Fisher Scientific, USA) were carried out to detect the surficial chemical properties of samples. The carbon (C) contents of samples were determined by a LECO-TC500-type C/S determinator.

RESULTS AND DISCUSSION

The synthesis processes of BN microspheres are shown and discussed in Figure 1, while the formation mechanism of the spherical precursor was proposed, as shown in Figure 2. The introduced methanol, which has nonpolarity, infinite mutual solubility to water, and chemical inertness to formaldehyde molecules without catalyzers, could accelerate the F-127 dissolution in the formaldehyde (formalin) solution at RT (step I in Figure 1). The accelerated dissolution may be due to the fact that the addition of methanol can change the separate aqueous atmospheres of formaldehyde solution into biconditional hydrophilic–lipophilic atmospheres, which can boost the solubility of the F-127. Also, methanol could efficiently suppress the metaformaldehyde precipitates self-polymerized from formaldehyde molecules.[17] This action ensures a kind of highly soluble adducts of x-methylol melamine formed from well-known reaction between formaldehyde and melamine molecules at 85 °C[18] (step II in Figure 1). The adducts were proposed to be 2,4-di(methoxymethyl)amino-1,3,5-triazine (DMAT) (Figure 2a), which belongs to one of the prepolymerized species of typical melamine–formaldehyde (MF) resin.

Owing to the hydrogen-bonding action, the un-methylated amino end of melamine and the hydrophilic end of F-127 form a bonding connection at 65 °C (see Figure 2a). At this time, the F-127 started to form transparent micelles in the mixed solution (Step III in Figures 1 and S1 in the Supporting Information (SI)). Due to the absence of oily components in the solution system, the as-architectured micelles presented a spherical shape formed with the lipophilic ends of F-127 as the sphere center and the hydrophilic ends of F-127 facing outward (Figure 2a). With slow hydrolysis of trimethyl borate to boric acid (BA) and methanol ($C_3H_9BO_3 + 3H_2O = H_3BO_3 + 3CH_3OH$), the hydroxyl ends of BA are also bonded to part of the hydrophilic ends of F-127's side chains by the hydrogen-bonding function. As a result, the DMAT/F-127/BA composite micelles gradually formed (see Figure 2b) and continuously self-assembled into microspherical particles. Simultaneously, a series of polycondensation reactions occurred among hydroxymethyl melamine and BA, forming a bulk of wet gel-like solidification interconnected with the self-assembled microspheres (step IV in Figures 1 and 2b). It can

https://doi.org/10.1021/acsomega.3c00313
ACS Omega 2023, 8, 15239−15248

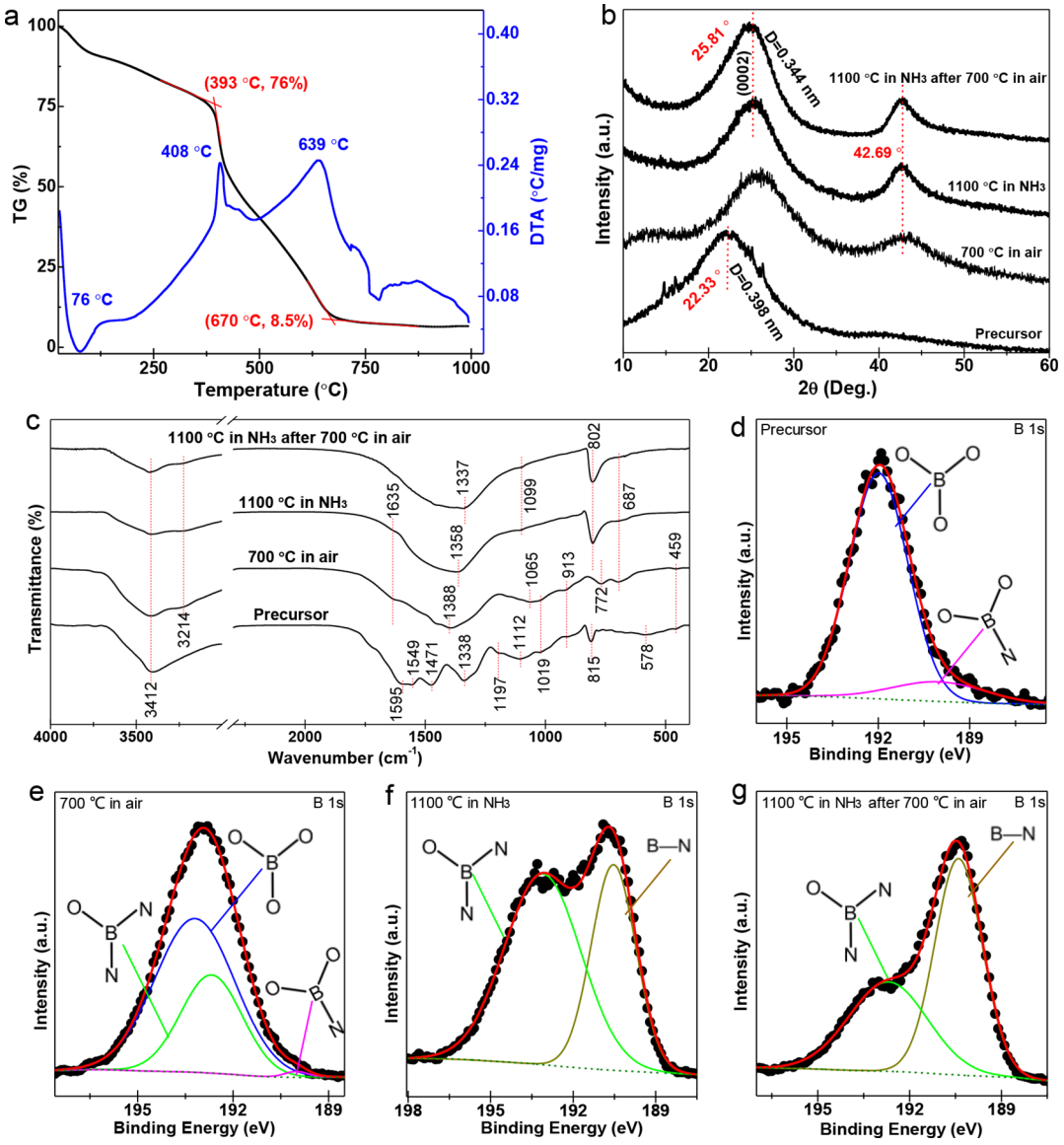

Figure 3. Characteristics of the samples. (a) TG-DTA curves of precursors measured under air flow. (b) XRD patterns. (c) FTIR spectra. (d–g) Fine-scanning B 1s spectra of XPS, and corresponding fitting peaks of their characteristic oxidation and nitridation states.

be seen that the F-127 plays an important role in self-assembling formation of polymerized spherical particles. There is no detectable trace of spherical morphology without adding F-127 (Figure S2 in the SI).

Interestingly, replacing trimethyl borate with BA would not bring about additional chemical reaction in the system, but direct addition of BA could lead to sudden pH turnabout in the solution system.[19] This mutation can sensitively induce the heterogeneous polymerization reaction in the colloidal system, which was more serious than that of BA from trimethyl borate hydrolysis (step III in Figure 1). In fact, although the additional methanol obtained from the pyrolysis of trimethyl borate could dilute the pH value caused by a certain amount of BA, the pH value would also be changed due to the BA production. However, the process of obtaining BA from the hydrolysis of trimethyl borate is relatively slow, which results in the overall uniformity of the overall pH value of the solution system induced by BA, so the polymerization was relatively uniform. With direct addition of BA, the obtained products also have a similar microspherical morphology. However, uncontrollability for the self-assembly and polymerization of DMAT/F-127/BA micelles were inevitably increased.

The wet gel bulk was heated at 200 °C to transfer into the precursor (step V in Figures 1 and 2c). The methanol, water, and unreacted formaldehyde molecules were removed from the solid bulk in the heating treatment. In addition, the hydrogen bonds between the F-127 and other ingredients within the as-formed DMAT/F-127/BA polymeric microspheres were broken. Subsequently, a possible condensation reaction between the exposed hydroxyl groups of BA and the naked amino groups of melamine was performed, thus forming a modest amount of O–B–N bonds in the precursor (Figure 2c). After this heating treatment, the polymerized gel solidification could be easily demoulded from the reaction vessels, and they became a dried bulk precursor (see the real photograph in step V in Figure 1). Maybe due to the existence of O–B–N networks, the spherical morphology could be well preserved after pyrolysis whether at 700 °C in air or directly at 1100 °C in ammonia (step VI in Figure 1).

https://doi.org/10.1021/acsomega.3c00313
ACS Omega 2023, 8, 15239–15248

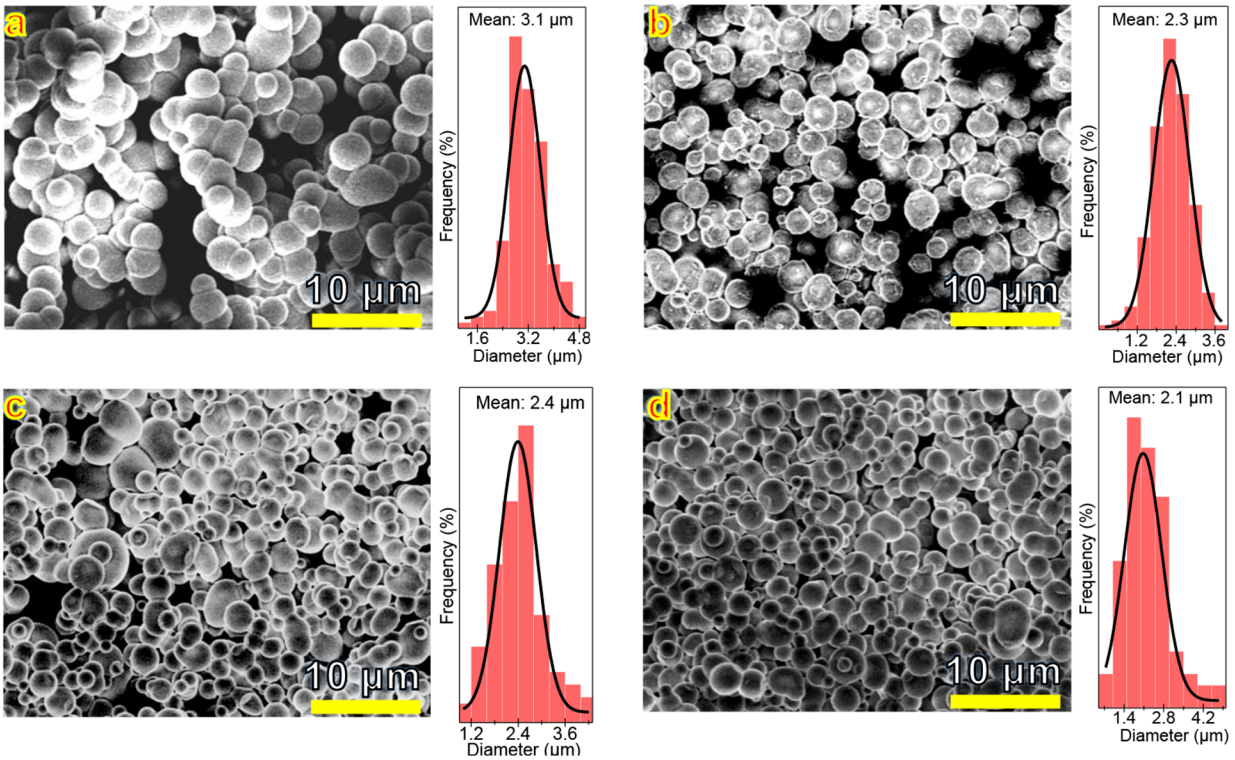

Figure 4. Morphologic properties of the samples illustrated by SEM images. (a) Microspherical precursor. (b) Pyrolyzed products at 700 °C in air. (c) Products pyrolyzed directly at 1100 °C in ammonia. (d) Products obtained at 1100 °C by ammonia-annealing of the intermediate which was prepyrolyzed at 700 °C in air.

During pyrolysis, an obvious transform from the precursor to the BN phase emerged (Figure 3). After pyrolysis at >670 °C in air, almost all the C impurities in the precursor can be removed (Figures 3a and S3 in the SI), leaving B-containing components of less than ∼8.5 wt %. From ∼393 to 670 °C, the C−N bonds of triazine-carbonitride heterocycles in the precursor were broken gradually. When it heated at ∼408 and 639 °C, the B−O also reacted with the decomposed C- and N-containing species to remove C-relation impurity as well as to make B−O nitridation to the BN phase. This tendency could be confirmed by the XRD results, which displayed that the typical steamed diffraction peak located nearby $2\theta = 22.33°$ transformed to two typical bulge peaks of $2\theta = 25$ and 42° (Figure 3b), which are attributed to the well-known amorphous/turbostratic BN phases.[20]

The product pyrolyzed at 700 °C in air has an increased B−N composition (Table S1 in SI) and ultra-low C impurity of 2.76 wt % (Table S2 in the SI). This result could also be verified by the disappearance of FTIR signature (Figure 3c). After pyrolysis at 700 °C in air, there appeared the B−N−B (772 cm^{-1}), O−B−N (913, 1019, and 1065 cm^{-1}), B−N (1388 cm^{-1}), B−O−B (687 and 578 cm^{-1}) and O−B−O (459 cm^{-1}) vibrations, with the disappearance of the precursor's C−N (1595, 1471, 1338 and 1112 cm^{-1}), C═N (1549 cm^{-1}), and triazine ring (815 cm^{-1}) vibrations which are always found in the typical MF-resin-based materials.[21] In addition, the coexistence of O−B−N and O−B−O vibrations (Figure 3c) as well as the presence of O−B−N and O−B−O bands in the XPS's fitting B 1s spectra (Figure 3d,e) could further support the proposed O−B−N bonding networks formed within the precursor microspheres (Figure 2c) due to the developed B−O nitridation during pyrolysis in air. Thus, this air-pyrolysis product is more like a kind of an intermediate of a BN microsphere with little C impurity but a lot of O content.

Further heating treatment of the intermediate at 1100 °C in ammonia could increase the BN phase similar to that of the product pyrolyzed directly at 1100 °C in ammonia (Figure 3b, c, f, g). Except for a certain amount of O−B−N (1099 cm^{-1}) and B−O (687 cm^{-1}) components, the two products have the dominant out-of-plane B−N−B bending (802 cm^{-1}) and in-plane B−N stretching (1358, or 1337 cm^{-1}) vibrations (FTIR of Figure 3c), which are very close to the typical characteristics of h-BN vibrations.[22] There were almost no detectable C-containing groups, which well agreed with the ultra-low C content detected to be only ∼0.48 wt % (Table S2 in the SI). These results indicate high-efficiency BN phase conversion during the intermediate's heating treatment at 1100 °C in ammonia (Figure 3f,g). From the B 1s spectra of XPS, it is obvious that the nitriding effect of the intermediate in ammonia-annealing treatment was better than that of direct pyrolysis under ammonia. For the products pyrolyzed directly in ammonia at 1100 °C and the products obtained from ammonia-annealing treatment of the intermediate at 1100 °C (Table S1 in SI), their atomic ratios of B/N/O are 1/0.7/0.5 and 1/0.7/0.3. The latter case contains much less O content of 19 wt % than the 28 wt % for the former. This may be due to the formation of richer O−B−N connection networks with ultra-low C impurity through the air-prepyrolysis of precursors in advance. These changes possibly make the subsequent B−O nitridation much easier for reducing the O content in the ammonia-annealing atmosphere. The difference is that pyrolysis in an inert atmosphere will lead to part the B−C bond which is difficult to be removed under the ammonia

https://doi.org/10.1021/acsomega.3c00313
ACS Omega 2023, 8, 15239−15248

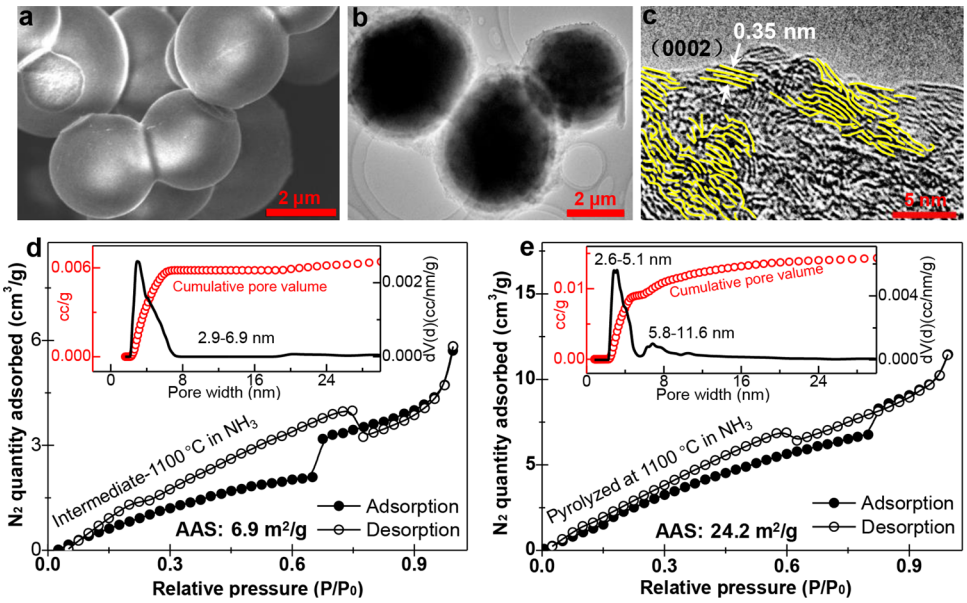

Figure 5. Structural characteristics and porous properties of the obtained boron nitride microspheres through ammonia-annealing treatment of the intermediate (first pyrolysis at 700 °C in air) at 1100 °C. (a) SEM image. (b, c) TEM and HR-TEM images. (d, e) N_2 adsorption−desorption isotherms and the insets corresponding to the summary for the QSDFT pore size distributions for the two kinds of BN microspheres obtained during different treatment processes.

treatment process, resulting in the product containing more C impurities and nonwhite body color characteristics.

After pyrolysis of the microspherical precursor, the obtained products maintained a good microspherical morphology (Figures 4 and S4−S7 in the SI). Although the different pyrolysis methods did not damage the spherical morphology of products, it affects the spherical size distribution. The size distribution of the spherical precursor ranges from 1 to 5 μm with an average value of 3.1 μm (Figures 4a and S4 in the SI). Due to the melting B−O networks tending to be densified along with the pyrolysis in air at 700 °C (great removal of carbonaceous constituents of precursors), the average diameter of the obtained intermediate microspheres was reduced to be ∼2.3 μm (Figures 4b and S5 in the SI), shrinking by 59% volume of the precursor spheres. However, the product obtained from direct pyrolysis at 1100 °C in ammonia (Figures 4c and S6 in the SI) has a slightly larger spherical size (mean distribution to be ∼2.4 μm) than those of the intermediate and its further ammonia-annealing products (mean of 2.1 μm) (Figures 4d and S7 in the SI). This change shows that the melting shrinkage of B−O in the entire ammonia environment is smaller than that of further ammonia-annealing treatment of the intermediate. The minimum spherical particles obtained from further ammonia-annealing treatment of the intermediate indicate that the continuous shrinkage will still occur in the B−O networks of the intermediate spheres.

The connection between precursor microspheres (Figure 4a) leads to similar surficial interconnection of the final BN microspheres (Figure 5a). A well-intact 3D framework in the obtained BN bulks (Figures S3−S8) was indirectly confirmed by the fact of the interconnected BN microspheres, also by a clear and crisp ceramic-like sound when they occasionally collided. The independent BN microparticles which still maintain a well spherical morphology can be easily attained through a simple crushing process to the as-formed BN bulks (Figure 5a,b). As shown in the above-tested/-analyzed results, a large number of C-, N-, H-, and O-containing components were gradually removed from the spherical precursor during the pyrolysis (Figure 3). Therefore, the final BN microspheres should have a high porosity. In fact, the ordering plane parts observed in Figure 5c seem to be the well-known turbostratic-type BN[20,23] (*t*-BN, with the d_{0002} value closer to 0.35 nm) (Figure 5c), which may be from the pore in the final BN spheres. However, these BN microspheres with a relatively low porosity do not follow those highly porous BN materials which generally have a lot of typical Y-form, helical screw, and radical-rich edge pores.[24−26]

In general, a polymerized material made of a regular micellar assembly should have well-ordered pore distribution when the surfactant F-127 is removed completely.[27,28] However, the relatively ordered pore characterization for our BN microspheres was not detected in the fine TEM scanning result and the small-angle XRD scanning pattern. Because the precursor contains a large number of B−O components, these B−O components will not only be partially nitrided during the heating process but also undergo glass transition with the increase of temperature. The formation of these vitrified states has efficient mass transfer and flow characteristics, resulting in the gradual destruction of regular pores formed by F-127 with the increase of temperature. Thus, it is almost difficult to detect regular pores in the final spherical BN products, which is consistent with the above-analyzed TEM results.

The N_2 adsorption isotherm is close to the type IV and/or VI for relatively low porosity[29] formed within the microspheres. The adsorption−desorption hysteresis loop is nearly attributed to the H1 and/or H2 type, which tends to be the pore characterization of accumulation or aggregation occurred from uniform spherical particles (Figure 5d,e).[30] The SSAs of the BN microspheres were very low. For example, through the multipoint BET method, the SSA of the BN spheres obtained from the ammonia-annealing intermediate (at 1100 °C) is calculated to be 6.9 m^2/g. Also, the SSA of the directly ammonia-pyrolyzing BN microspheres (at 1100 °C) is 24.2

https://doi.org/10.1021/acsomega.3c00313
ACS Omega 2023, 8, 15239−15248

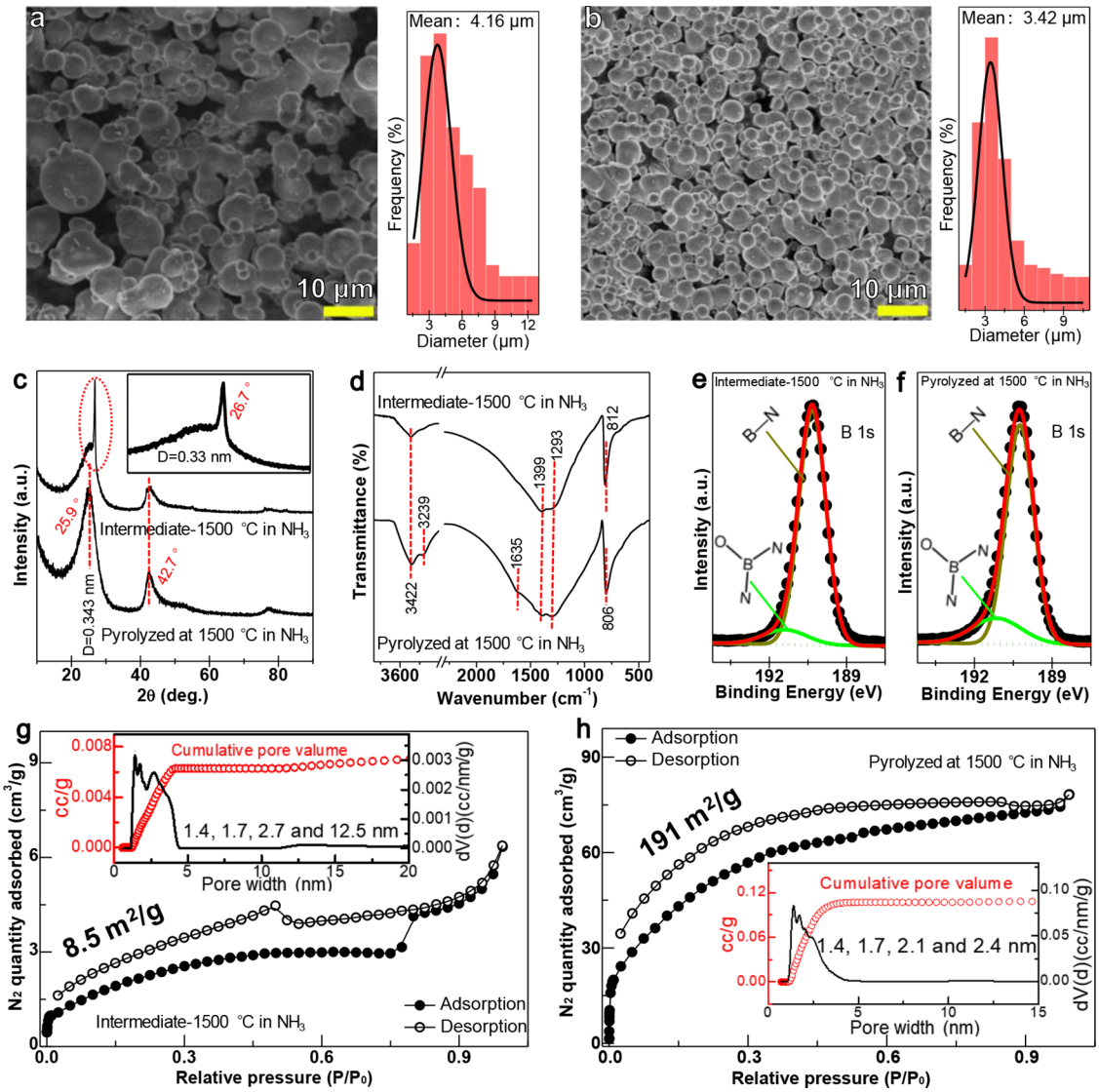

Figure 6. Characteristics of samples obtained at 1500 °C in ammonia atmospheres. (a, b) Morphologic properties of the samples illustrated by SEM images: (a) showing the sample pyrolyzed directly at 1500 °C in ammonia and its corresponding statistics of particle size distribution; (b) showing the samples obtained by the ammonia-annealing treatment of the intermediate at 1500 °C, and its corresponding statistics of particle size distribution. (c) XRD patterns of the two kinds of samples. (d) FTIR spectra of the two kinds of samples. (e, f) Fine-scanning XPS spectra of B 1s for the two kinds of samples. (g, h) (d, e) N_2 adsorption−desorption isotherms and the insets corresponding to the summary for the QSDFT pore size distributions for the two kinds of BN microspheres obtained during different treatments at 1500 °C.

m^2/g. In fact, BN spheres pyrolyzed directly with ammonia show a slightly reduced pore size in the range of 2.6−5.1 nm compared to the range of 2.9−6.9 nm of the ammonia-treated intermediate and show a significantly increased pore distribution scope of 5.8−11.6 nm.

The adsorption−desorption isothermal curve of precursors shows similar shapes and trends (Figure S9), also resulting in a very low SSA value. We think that this type of isothermal curve is very consistent with the microsphere formation from the self-assembly of smaller spheres. Referring to the low SSA and adsorption−desorption characteristics similar to the intermediate (Figure S10), the reason for the low SSA caused by air-pyrolysis treatment at 700 °C is that the microspheres with self-assembled structures may be more likely to cause pore collapse under the continuous mass transfer and melting state of the high-temperature B−O species, thus limiting the occurrence of high porosity with removal of F-127. However, it was interesting that the precursor particles obtained by partially replacing melamine with dicyandiamide could still maintain the microspherical morphology (see Figure S11). After direct ammonia-pyrolysis treatment at 1100 °C, the surface of the obtained BN microspheres becomes very rough, and its SSA could reach 1231 m^2/g with dominated pore size distribution of 0.92 and 3.21 nm, and its total pore volume could reach 0.845 cm^3/g (Figure S12).

At a higher target temperature of 1500 °C, the obtained BN particles still present a microspherical morphology (Figure 6a,b). However, there are different size distributions for different processes of the direct ammonia-pyrolysis precursor and further ammonia-annealing intermediate. For instance, the particle size (mean of 4.16 μm) of BN microspheres obtained by direct ammonia-pyrolysis treatment at 1500 °C (Figure 6a) is much larger than that (mean of 3.42 μm) of the ammonia-annealing intermediate at 1500 °C (Figure 6b). The latter (Figure 6b) has much more uniform size distribution. Such increased size for the direct ammonia-pyrolysis process was

https://doi.org/10.1021/acsomega.3c00313
ACS Omega 2023, 8, 15239−15248

mainly caused by a more easily combined and sintered B−O component between/among the connected spheres due to more O content that existed within the direct pyrolysis samples in the range of 1100−1500 °C (Figure 3f,g, and Tables S1−S3 in the SI).

In addition, the XRD and FTIR results also illustrate that the ammonia-annealing intermediate has more improved BN characteristics and phase (Figure 6c,d). For example, compared with the BN microspheres obtained by direct pyrolysis in ammonia at 1100 °C, the XRD pattern center of the (0002) crystal plane for the BN microspheres with ammonia-pyrolysis at 1500 °C was moved to 25.9°. At the same time, the crystallinity of BN microspheres obtained from the ammonia-annealing intermediate at 1500 °C is highly improved superior to that obtained from ammonia-annealing at 1100 °C, which displays a significantly enhanced (0002) crystal plane located at $2\theta = 26.7°$ corresponding to the (0002) plane spacing of 0.33 nm (inset of Figure 6d) as well as a well-crystalized h-BN phase.[31] In the products obtained at 1500 °C, the obvious B−O vibration similar to that obtained at 1100 °C (see Figure 3c) can hardly be detected in the FTIR, indicating that the BN phase within the microspheres is gradually purified with the increase of treatment or pyrolysis temperature, especially for the products generated from the ammonia-annealing intermediate. For example, compared with the BN microspheres produced by direct pyrolysis of ammonia at 1500 °C, it was worth noting that the vibration at 3239 cm^{-1} which belongs to the −OH group has disappeared for the BN microspheres from intermediates treated with ammonia at 1500 °C. In addition, the 1635 cm^{-1} vibrations for the C−N bond disappeared in the final BN microsphere obtained from the ammonia-annealing intermediate either at 1100 or at 1500 °C (Figures 3c and 6d).

In addition, the fine-scanning B 1s spectra of XPS also illustrate that the BN microspheres based on the ammonia-annealing intermediate at 1500 °C show more significant BN characterization and less B−O components than that of the direct ammonia-pyrolysis treatment of the precursor (Figure 6e,f), indicating the obvious advantage of effective removal of C impurities in BN microspheres by means of the prior air-pyrolysis process. It is worth noting that the adsorption−desorption curve of BN microspheres (Figure 6g) subjected to the ammonia-annealing intermediate at 1500 °C is very similar to the results of the direct ammonia-pyrolysis precursor and/or the ammonia-annealing intermediate at 1100 °C (Figure 5d,e), showing typical pore characteristics caused by spherical particle aggregation or accumulation. These BN microspheres still maintain a low SSA value of 8.5 m^2/g. However, its characteristics are significantly different from BN microspheres directly subjected to the ammonia-pyrolysis process at 1500 °C (Figure 6h), which shows the near type I isothermal curve and type H4 isothermal loop for typical mix-existence of micropores and narrow-crack pores similar to some kinds of activated carbon materials. Moreover, the directly pyrolyzed product has a weak shrinking trend toward the pore size. Compared with 1100 °C, the increased pore distribution may be due to the formation of more areas in BN microspheres that could not be well crystallized in time after the high B−O composition with the ammonia-nitridation reaction when higher than 1100 °C. These areas usually show a higher microlevel and narrow-crack pores made of the low-crystalline *t*-BN structure.[24−26] Thus, more uniform size distribution and higher BN phase of BN microspheres are easily achieved in the ammonia-annealing treatment of the intermediate.

CONCLUSIONS

In summary, we have successfully developed a new synthetic route to BN microspheres through two main processes including the facile self-assembling polymerization of the microspherical precursor and the controllable pyrolysis and annealing of the microsphere precursor in air and/or in ammonia atmospheres. The surfactant F-127 played an important role in self-assembling DMAT/F-127/BA micelles and the polymerized precursor microspheres due to its highly hydrogen-bonding action and distinctly hydrophilic/hydrophobic ends. Because of the existence of O−B−N bonding networks within the microspherical precursor, the spherical morphology could be well preserved through air-pyrolysis at 700 °C or direct ammonia-pyrolysis at 1100 and/or 1500 °C. It is obvious that more uniform size distribution of BN microspheres and higher BN phase transformation with the BN microspheres were easily achieved by the further ammonia-annealing treatment of the intermediate at 1100 and/or 1500 °C, compared to those of direct ammonia-pyrolysis cases. In addition, we found that after partially replacing melamine with dicyandiamide, the SSA and pore sizes of the BN microspheres could be regulated and controlled to exceed 1000 m^2/g. We believe that this commercializable technology for spherical BN preparation will promote the further extensive application of high-density h-BN ceramics, well-dispersed BN/polymer composites, and porous BN bulk materials.

ASSOCIATED CONTENT

Supporting Information

The Supporting Information is available free of charge at https://pubs.acs.org/doi/10.1021/acsomega.3c00313.

> Transparent colloidal system at 65 °C for obvious Tyndall effect; SEM of precursors with and without adding the F-127; products from the air-pyrolysis process at 550 °C; measured atomic ratio of B/N/O and O contents; contents of carbon impurity; low-resolution SEM images for documenting the uniformity of the precursor and BN microspheres; XPS data and analysis for the products obtained at 1500 °C; and nitrogen adsorption−desorption curves coupled with pore analysis for the precursor and the products obtained at 1500 and 700 °C (PDF)

AUTHOR INFORMATION

Corresponding Author

Yanming Xue − *School of Materials Science and Engineering and Hebei Key Laboratory of Boron Nitride Micro- and Nano-Materials, Hebei University of Technology, Tianjin 300130, P.R. China;* orcid.org/0000-0003-1061-229X; Email: ym.xue@hebut.edu.cn

Authors

Zexia Li − *School of Materials Science and Engineering and Hebei Key Laboratory of Boron Nitride Micro- and Nano-Materials, Hebei University of Technology, Tianjin 300130, P.R. China;* orcid.org/0000-0002-8622-4958

Jingwen Yang − *School of Materials Science and Engineering and Hebei Key Laboratory of Boron Nitride Micro- and*

https://doi.org/10.1021/acsomega.3c00313
ACS Omega 2023, 8, 15239−15248

Nano-Materials, Hebei University of Technology, Tianjin 300130, P.R. China; orcid.org/0000-0002-8585-8801

Hejun Gao − *School of Materials Science and Engineering and Hebei Key Laboratory of Boron Nitride Micro- and Nano-Materials, Hebei University of Technology, Tianjin 300130, P.R. China;* orcid.org/0000-0002-3250-0398

Jiaxiao Qiao − *School of Materials Science and Engineering and Hebei Key Laboratory of Boron Nitride Micro- and Nano-Materials, Hebei University of Technology, Tianjin 300130, P.R. China;* orcid.org/0000-0003-1171-6314

Wei Qiao − *School of Materials Science and Engineering and Hebei Key Laboratory of Boron Nitride Micro- and Nano-Materials, Hebei University of Technology, Tianjin 300130, P.R. China;* orcid.org/0000-0003-2371-7111

Peng Wang − *School of Materials Science and Engineering and Hebei Key Laboratory of Boron Nitride Micro- and Nano-Materials, Hebei University of Technology, Tianjin 300130, P.R. China;* orcid.org/0000-0002-1695-3602

Jun Zhang − *School of Materials Science and Engineering and Hebei Key Laboratory of Boron Nitride Micro- and Nano-Materials, Hebei University of Technology, Tianjin 300130, P.R. China;* orcid.org/0000-0002-4958-6925

Chengchun Tang − *School of Materials Science and Engineering and Hebei Key Laboratory of Boron Nitride Micro- and Nano-Materials, Hebei University of Technology, Tianjin 300130, P.R. China;* orcid.org/0000-0002-1484-789X

Complete contact information is available at: https://pubs.acs.org/10.1021/acsomega.3c00313

Notes

The authors declare no competing financial interest.

■ ACKNOWLEDGMENTS

Y.M.X. receives and appreciates the financial support from the National Natural Science Foundation of China (Grant No. 51802073), from Hebei province eighth batch of "100 people plan" project (No. E2018050008), from the Natural Science Foundation of Hebei province (Grant No. E2020202145), and from the project of the Science and Technology Plan of Tianjin (The Natural Science Foundation of Tianjin) (Grant No. 22JCYBJC00230).

■ REFERENCES

(1) Paine, R. T.; Narula, C. K. Synthetic routes to boron nitride. *Chem. Rev.* **1990**, *90*, 73−91.

(2) Lindquist, D. A.; Kodas, T. T.; Smith, D. M.; Xiu, X. M.; Hietala, S. L.; Paine, R. T. Boron Nitride Powders Formed by Aerosol Decomposition of Poly(borazinylamine) Solutions. *J. Am. Ceram. Soc.* **1991**, *74*, 3126−3128.

(3) Hubácek, M.; Ueki, M. Effect of the orientation of boron nitride grains on the physical properties of hot-pressed ceramics. *J. Am. Ceram. Soc.* **1999**, *82*, 156−160.

(4) Aghajani, A.; Ehsani, M.; Khajavi, R.; Kalaee, M.; Zaarei, D. Thermally conductive and mechanically strengthened bio-epoxy/boron nitride nanocomposites: the effects of particle size, shape, and combination. *Polym. Compos.* **2022**, *43*, 9027.

(5) Jiang, H. B.; Mateti, S.; Cai, Q. R.; Shao, H.; Huang, S. M.; Wu, Z. S.; Zhi, C. Y.; Chen, Y. L. Quasi-isotropic thermal conductivity of polymer films enhanced by binder-free boron nitride spheres. *Compos. Sci. Technol.* **2022**, *230*, No. 109769.

(6) Vatanpour, V.; Mehrabani, S. A. N.; Keskin, B.; Arabi, N.; Zeytuncu, B.; Koyuncu, I. A comprehensive review on the application of boron nitride nanomaterials in membrane fabrication and modification. *Ind. Eng. Chem. Res.* **2021**, *60*, 13391−13424.

(7) Tang, C. C.; Bando, Y.; Golberg, D. Large-scale synthesis and structure of boron nitride sub-micron spherical particles. *Chem. Commun.* **2002**, 2826−2827.

(8) Tang, C. C.; Bando, Y.; Huang, Y.; Zhi, C. Y.; Golberg, D. Synthetic routes and formation mechanisms of spherical boron nitride nanoparticles. *Adv. Funct. Mater.* **2008**, *18*, 3653−3661.

(9) Wood, G. L.; Janik, J. F.; Visi, M. Z.; Schubert, D. M.; Paine, R. T. New borate precursors for boron nitride powder synthesis. *Chem. Mater.* **2005**, *17*, 1855−1859.

(10) Wang, Y. T.; Yamamoto, Y.; Kiyono, H.; Shimada, S. Effect of ambient gas and temperature on crystallization of boron nitride spheres prepared by vapor phase pyrolysis of ammonia borane. *J. Am. Ceram. Soc.* **2009**, *92*, 787−792.

(11) Pruss, E. A.; Wood, G. L.; Kroenke, W. J.; Paine, R. T. Aerosol assisted vapor synthesis of spherical boron nitride powders. *Chem. Mater.* **2000**, *12*, 19−21.

(12) Terrones, M.; Charlier, J. C.; Gloter, A.; Cruz-Silva, E.; Terrés, E.; Li, Y. B.; Vinu, A.; Zanolli, Z.; Dominguez, J. M.; Terrones, H.; Bando, Y.; Golberg, D. Experimental and theoretical studies suggesting the possibility of metallic boron nitride edges in porous nanourchins. *Nano Lett.* **2008**, *8*, 1026−1032.

(13) Han, W. Q.; Wang, J. P.; Liu, S. C.; Ge, C. H.; Gao, S. W.; Song, B.; Wang, J.; Zhang, X. D. Spectral properties of spherical boron nitride prepared using carbon spheres as template. *Ceram. Int.* **2017**, *43*, 3569−3575.

(14) Zhang, N.; Liu, H.; Kan, H. G.; Wang, X. Y.; Long, H. B.; Zhou, Y. H. The preparation of high-adsorption, spherical, hexagonal boron nitride by template method. *J. Alloys Compd.* **2014**, *613*, 74−79.

(15) Zhang, N.; Liu, H.; Kan, H. G.; Wang, X. Y.; Long, H. B.; Zhou, Y. H. The influence of surface-active agent on the micro-morphology and crystallinity of spherical hexagonal boron nitride. *J. Nanosci. Nanotechnol.* **2015**, *15*, 6218−6224.

(16) Zhang, T.; Wen, G.; Xia, L.; Huang, X. X.; Zhong, B.; Zhang, X. D.; Bai, H. W.; Yu, H. M. Synthesis of BN microspheres with high-purity via a polymer-chemical route. *Scr. Mater.* **2010**, *63*, 415−417.

(17) Albrecht, L.; Boyd, R. J. Atomic energy analysis of cooperativity, anti-cooperativity, and non-cooperativity in small clusters of methanol, water, and formaldehyde. *Comput. Theor. Chem.* **2015**, *1053*, 328−336.

(18) Leskovšek, M.; Kortnik, J.; Elesini, U. S.; Šumiga, B. Characterisation of melamine formaldehyde microspheres synthesized with prolonged microencapsulated reaction time. *J. Polym. Eng.* **2022**, *42*, 288−297.

(19) Bai, C.; Liu, H. N.; Liu, Z.; Ye, X. S.; Zhang, H. F.; Li, J.; Wu, Z. J. Reactions of boric acid/borax with polyhydroxyl compounds: solution pH, conductivity and Raman spectroscopy. *J. Salt Lake Res.* **2020**, *28*, 56−64.

(20) Gao, S. T.; Li, B.; Zhang, C. R.; Li, D.; Liu, R. J.; Wang, S. Q. Chemical vapor deposition of pyrolytic boron nitride ceramics from single source precursor. *Ceram. Int.* **2017**, *43*, 10020−10025.

(21) Seidl, R.; Weiss, S.; Kessler, R. W.; Kessler, W.; Zikulnig-Rusch, E. M.; Kandelbauer, A. Prediction of residual curing capacity of melamine-formaldehyde resins at an early stage of synthesis by in-line FTIR Spectroscopy. *Polymer* **2021**, *13*, 2541.

(22) Cao, C. C.; Yang, J. W.; Fu, K.; Zhai, Q. H.; Zhou, Z.; Ji, J. W.; Ma, Y. H.; Zhou, M.; Xue, Y. M.; Tang, C. C. Hierarchically porous boron nitride foams for multifunctional bulk adsorbents. *Chem. Eng. J.* **2021**, *422*, No. 129896.

(23) Toyofuku, N.; Yamasaki, N.; Kodera, Y.; Ohyanagi, M.; Munir, Z. A. Turbostratic boron nitride consolidated by SPS. *J. Ceram. Soc. Jpn.* **2009**, *117*, 189−193.

(24) Xue, Y. M.; Dai, P. C.; Jiang, X. F.; Wang, X. B.; Zhang, C.; Tang, D. M.; Weng, Q. H.; Wang, X.; Pakdel, A.; Tang, C. C.; Bando, Y.; Golberg, D. Template-free synthesis of boron nitride foam-like porous monoliths and their high-end applications in water purification. *J. Mater. Chem. A* **2016**, *4*, 1469−1478.

(25) Weng, Q. H.; Wang, X. B.; Zhi, C. Y.; Bando, Y.; Golberg, D. Golberg, Boron nitride porous microbelts for hydrogen storage. *ACS Nano* **2013**, *7*, 1558−1565.
(26) Cao, C. C.; Yang, J. W.; Yan, S.; Bai, W. J.; Ma, Y. H.; Xue, Y. M.; Tang, C. C. Photoelectric and magnetic properties of boron nitride nanosheets with turbostratic structure and oxygen doping. *2D Mater.* **2022**, *9*, No. 015014.
(27) Tian, W. J.; Zhang, H. Y.; Duan, X. G.; Sun, H. Q.; Shao, G. S.; Wang, S. B. Porous carbons: Structure-oriented design and versatile applications. *Adv. Funct. Mater.* **2020**, *30*, No. 1909265.
(28) Roberts, A. D.; Li, X.; Zhang, H. F. Porous carbon spheres and monoliths: morphology, pore size tuning and their applications as Li-ion battery anode materials. *Chem. Soc. Rev.* **2014**, *43*, 4341−4356.
(29) Cychosz, K. A.; Thommes, M. Progress in the physisorption characterization of nanoporous gas storage materials. *Engineering* **2018**, *4*, 559−566.
(30) Neimark, A. V.; Ravikovitch, P. I.; Vishnyakov, A. Adsorption hysteresis in nanopores. *Phys. Rev. E* **2000**, *62*, R1493.
(31) Xue, Y. M.; Zhou, X.; Zhan, T. Z.; Jiang, B. Z.; Guo, Q. S.; Fu, X. W.; Shimamura, K.; Xu, Y. B.; Mori, T.; Dai, P. C.; Bando, Y.; Tang, C. C.; Golberg, D. Densely interconnected porous BN frameworks for multifunctional and isotropically thermoconductive polymer composites. *Adv. Funct. Mater.* **2018**, *28*, No. 1801205.

https://doi.org/10.1021/acsomega.3c00313
ACS Omega 2023, 8, 15239−15248